Supporting Information

Microscopic temperature-dependent structural dynamics in polymer nanocomposites: role of graft-matrix chain interfacial entropic effect

Aparna Swain,[†,‖] Nimmi Das A,[†,‡,¶,‖] Victoria García Sakai,[§] and J. K. Basu[*,†]

†*Department of Physics, Indian Institute of Science Bangalore, 560012, India.*

‡*Department Physik, Universität Siegen, Walter-Flex-Strasse 3, 57072 Siegen, Germany.*

¶*Deutsches Elektronen-Synchrotron, Notkestrasse 85, 22607 Hamburg, Germany.*

§*ISIS Neutron and Muon Source, Rutherford Appleton Laboratory, Chilton, Oxfordshire OX11 0QX, UK*

‖*These two authors contributed equally to this work.*

E-mail: basu@iisc.ac.in

This supporting document includes information on sample preparation, characterization of deuterated-polystyrene grafted nanoparticles (DPGNPs), estimation of glass transition temperature, analysis of QENS data, extraction of relaxation time, mean square displacement, and non-Gaussian parameter.

Sample preparation

Deuterated-polystyrene grafted gold nanoparticles (DPGNPs) are synthesized by following a grafting-to method.[1,2] Deuterated thiol-terminated polystyrene (DPST) with molecular weight $M_g = 5$ kDa bought from "Polymer source" is used for grafting. DPST is dissolved and stirred overnight in distilled tetrahydrofuran (THF). Gold(III) chloride trihydrate (HAuCl4.3H2O) is dissolved separately in THF mixed with DPST solution and kept stirring for 30 minutes in an ice bath. A reducing agent superhydride is added to this mixture drop by drop, which leads to the reduction of gold ions and formation of Au nanoparticles (NPs) with simultaneous grafting of DPST chains eventually resulting in the formation of polystyrene grafted nanoparticles. After stirring the solution for 90 minutes, a few milliliters of ethanol is added to terminate the chemical reaction. The addition of ethanol selectively precipitates grafted DPST chains. DPGNPs settle down during centrifugation and supernatant liquid with ungrafted chains is disposed . Ungrafted polymer chains are completely removed by following this selective precipitation procedure 4-5 times. Finally, the precipitated DPGNPs are dissolved in THF and vacuum dried for 2-3 hours.

Characterization of DPGNPs

DPGNPs are characterized using transmission electron microscopy (TEM), small-angle X-ray scattering (SAXS), and thermo gravimetric analysis (TGA). The size of the Au core of DPGNP is estimated from TEM images as shown in Fig. S1(a-b). The total size of the DPGNPs is determined from SAXS measurements (Bruker Nanostar, USA) with an incident X-ray of wavelength of 1.54 $\mathring{A}^{-1}$. The diameter of DPGNP is extracted from the structure factor peak position as depicted in Fig. S1 (c). The weight fraction of Au core in DPGNPs is calculated from TGA (Figure S1d). Glass transition temperature (T_g) of DPGNPs and matrix polymers was measured using differential scanning calorimetry (DSC).

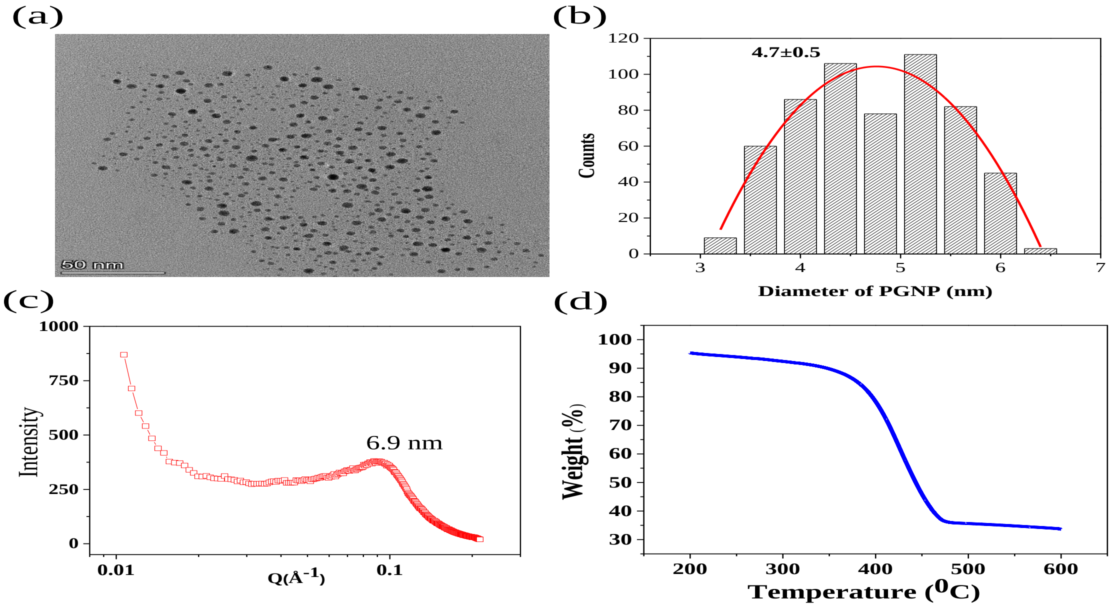

Fig. S1: a) The TEM image of DPGNP, b) the corresponding size distribution histogram of DPGNP, c) SAXS data of DPGNP, d) TGA data of the DPGNP samples.

Preparation of PNC

To create PNC samples with different f (graft to matrix molecular weight ratio) values, we have mixed DPGNPs in a hydrogenated polystyrene matrix with molecular weights 20kDa and 100kDa. For this, PS and DPGNPs are dissolved in toluene separately and stirred overnight. After overnight stirring, PS and DPGNP solutions are mixed in a certain ratio to get the final volume fraction of gold in PNC solution as 15%. Polymer nanocomposite solutions are stirred overnight to ensure homogeneous mixing. Then we drop-cast the solution on a Teflon disc and kept drying for 2 days. All samples are annealed at 145 °C (well above T_g = 100 °C of PS) in vacuum of 5 $\times 10^{-5}$ mbar for 12 hours.

Thickness of Bulk films and Lateral dispersion of DPGNPs from SEM

The thickness of the PNC film is estimated to be 120 μm (Fig. S2 (c) and (d)) using crossectional scanning electron microscopy (SEM) imaging. The dispersion of nanoparticles in PNCs is visualized using SEM as shown in Fig. S2 (a) and (b). To quantify the DPGNP dispersion in PNCs further, we have collected SAXS data on the PNCs as shown in Fig. S3. From the SAXS profiles (Fig. S3), the slope of L-PNC and S-PNC was quantified at a low Q regime to quantify the mass fractional dimension (d_m).[3] This quantity provides the quantification of the dispersion of L-PNC and S-PNC. It is clear that the d_m value for L-PNC is less than S-PNC which is clear quantifiable information that L-PNCs are much better dispersed compared to S-PNCs.

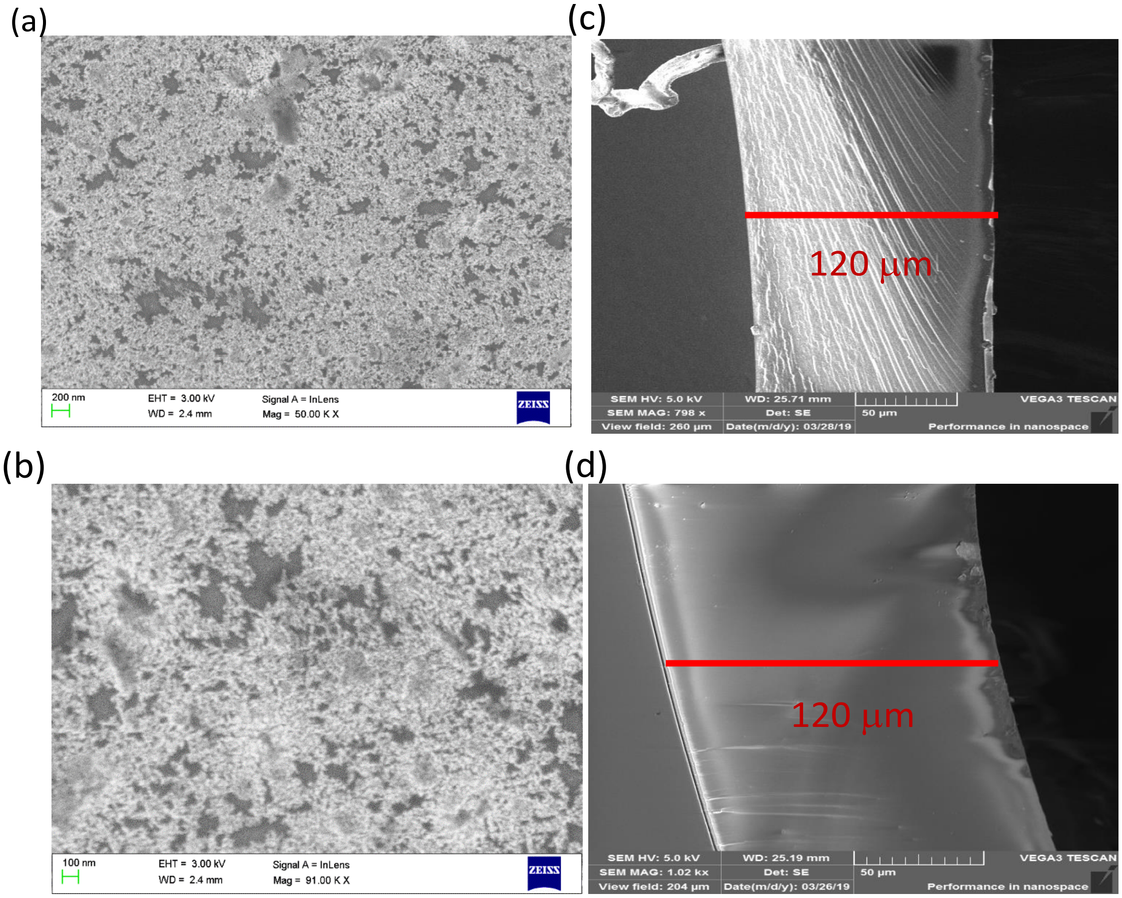

Fig. S2: SEM image of (a) L-PNC and (b) S-PNC. Crossectional SEM image used for thickness estimation of (c) L-PNC, and (d) S-PNC.

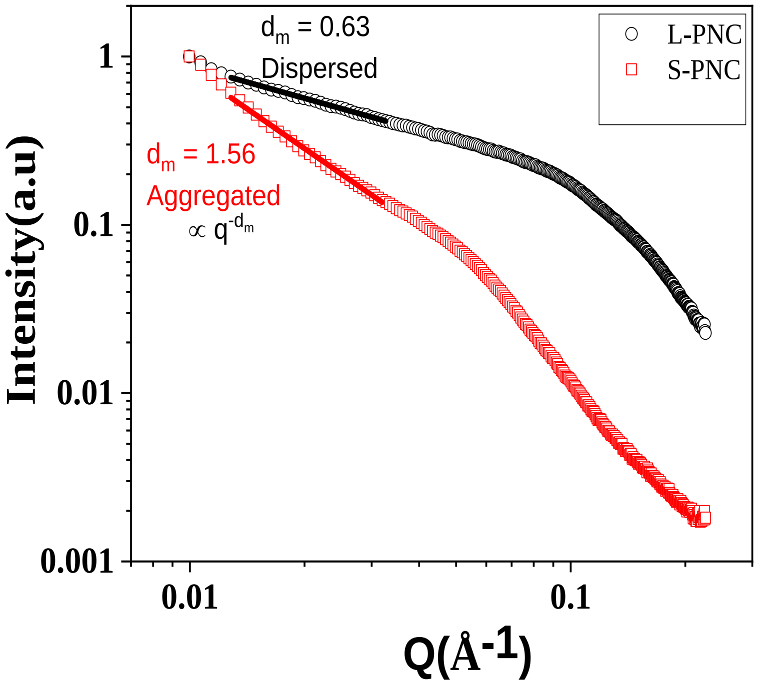

Fig. S3: The SAXS data plot of log I vs log Q to Mass fractal dimension (dm) for L-PNC and S-PNC.

Glass transition temperature T_g from DSC

We performed DSC measurements to find the glass transition temperature, T_g of PS and PNC samples. In Fig. S4 (a-d) the black and red straight lines trace the different slopes on DSC curves allowing us to visualize the T_g of PS and PNC samples respectively.

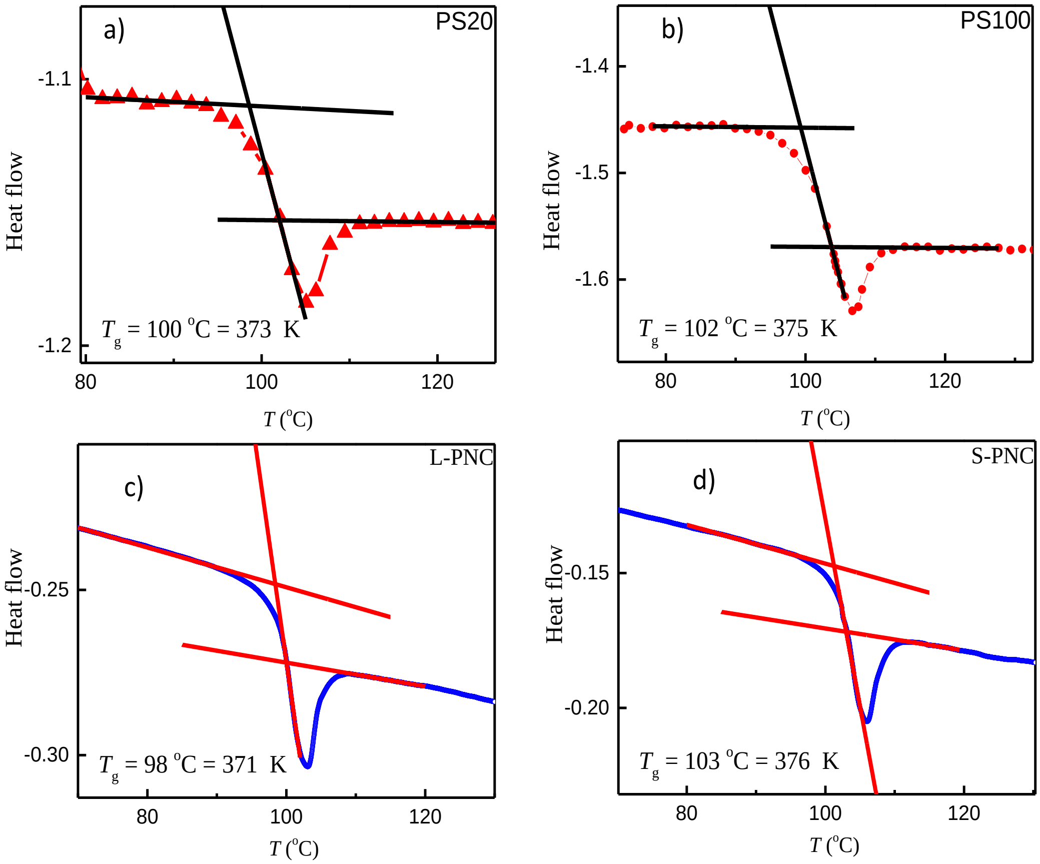

Fig. S4: Bulk T_g determination of a) PS20 b) PS100, c) L-PNC, and d) S-PNC from DSC curves using 3 slope method. Black and red straight lines trace the different slopes on DSC curves allowing us to visualize the T_g of PS and PNC samples respectively.

Study of dynamics using QENS

Quasi-elastic neutron scattering (QENS) measurements on annealed PNC and pure PS films give information on the dynamical aspects of samples. QENS experiments were carried out using the IRIS spectrometer at the ISIS neutron and muon facility at RAL, United Kingdom. IRIS is a backscattering spectrometer that uses pyrolitic graphite. Using the instrument in the offset mode with (002) reflection, the energy resolution of the instrument is 18.3 μeV (full width at half-maximum) and the energy transfer range is -0.3 to 1.0 meV. The wave-vector (Q) transfer range of the spectrometer is between 0.4 and 1.8 $\mathring{A}^{-1}$. QENS experiments on

PNCs were carried out at temperatures in the range of 300 - 450 K. For the instrument resolution, QENS measurements were carried out on a standard vanadium sample. The samples were placed in an annular aluminum can with an internal spacing of 1 mm to minimize multiple scattering and have reasonable measuring statistics. MANTID software[4] was used to carry out standard data reduction including background subtraction and detector efficiency corrections. The QENS spectra for PS20 for $Q = 1.1\text{Å}^{-1}$ at different temperatures are shown in Fig. S5. As the temperature increases, the broadening of the spectra increases.

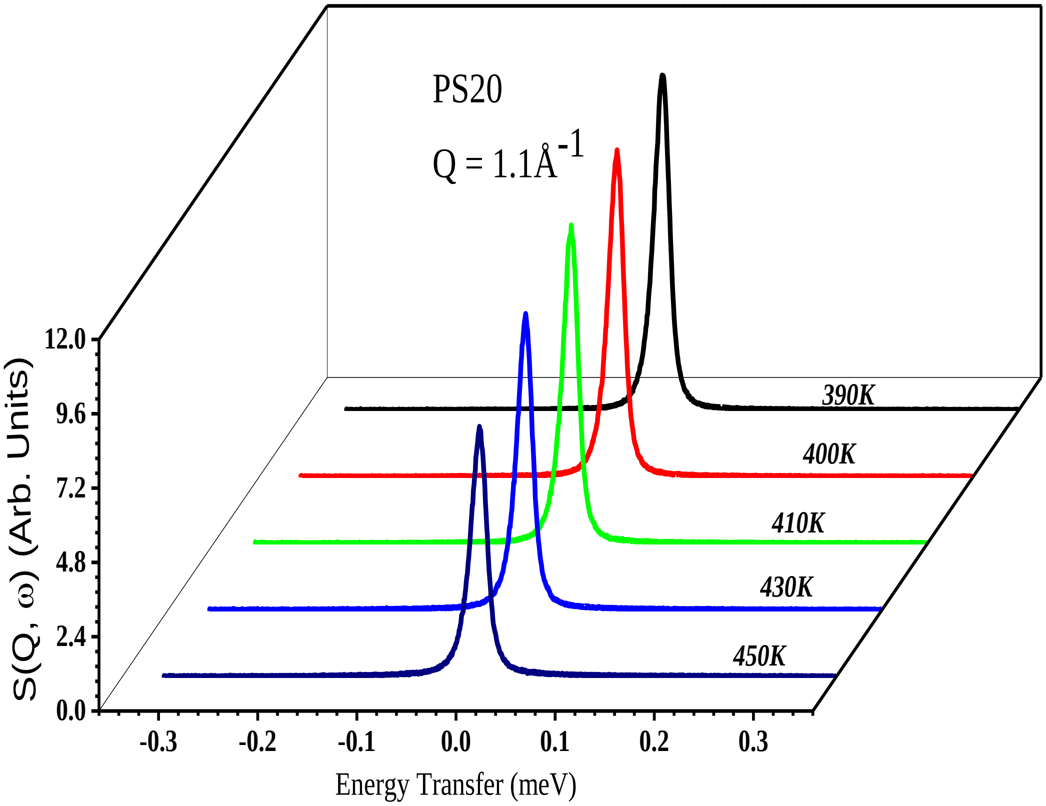

Fig. S5: The S(Q, ω) of PS20 for different temperatures at $Q = 1.1\,\text{Å}^{-1}$. The broadening increases with an increase in temperature.

Estimation of crossover wave vector $Q_\mathbf{c}$

To extract crossover wavevector, Q_c, we have fitted power-law functions ($\tau_\mathrm{kww} \approx Q^a$) at low-$Q$ and high Q regions. Then power-law fits are extrapolated to intermediate Q and the intersection point of these fits gives Q_c (Fig. S6). The deviation of τ is more for L-PNC as compared to S-PNC with pristine polymer.

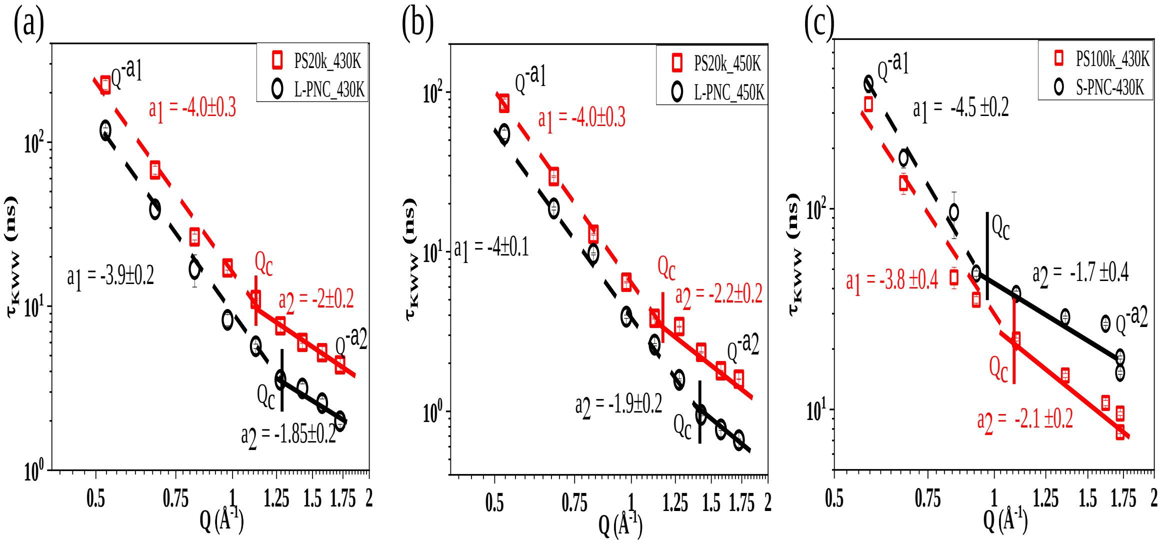

Fig. S6: τ_kww vs Q (log-log scale) of a) L-PNC and PS20 at $T = 430$ K, b) for L-PNC and PS20 at $T = 450$ K, and c) S-PNC and PS100 at $T = 430$ K. The power-law exponents (a_1 and a_2 at low-Q and high Q regions respectively) are mentioned in the figure. The cross-over wavevector, Q_c is denoted by a short vertical line.

The shift factor used in the main text Fig. 5(c-d) is shown in Figure S7.

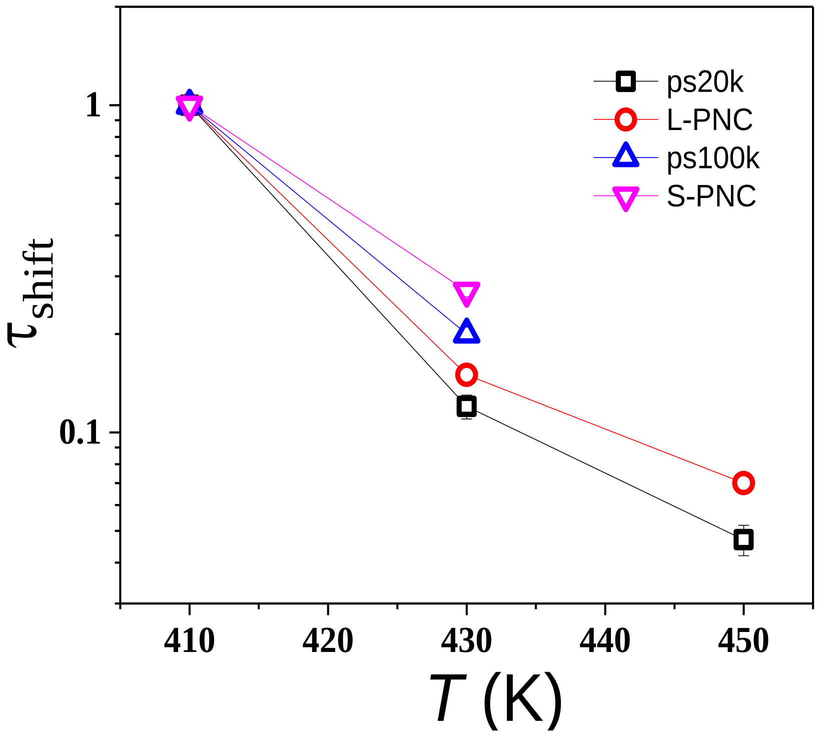

Fig. S7: τ_{shift} vs T for all samples.

Jump diffusion model to extract the segmental length and relaxation time

The relaxation time data are fitted using a jump-diffusion model proposed by Arbe et al.[5,6] for polymer melts as depicted in Fig. S8. From the fits, jump length l_0 and jump relaxation time τ_0 are extracted and their values are given in main text.

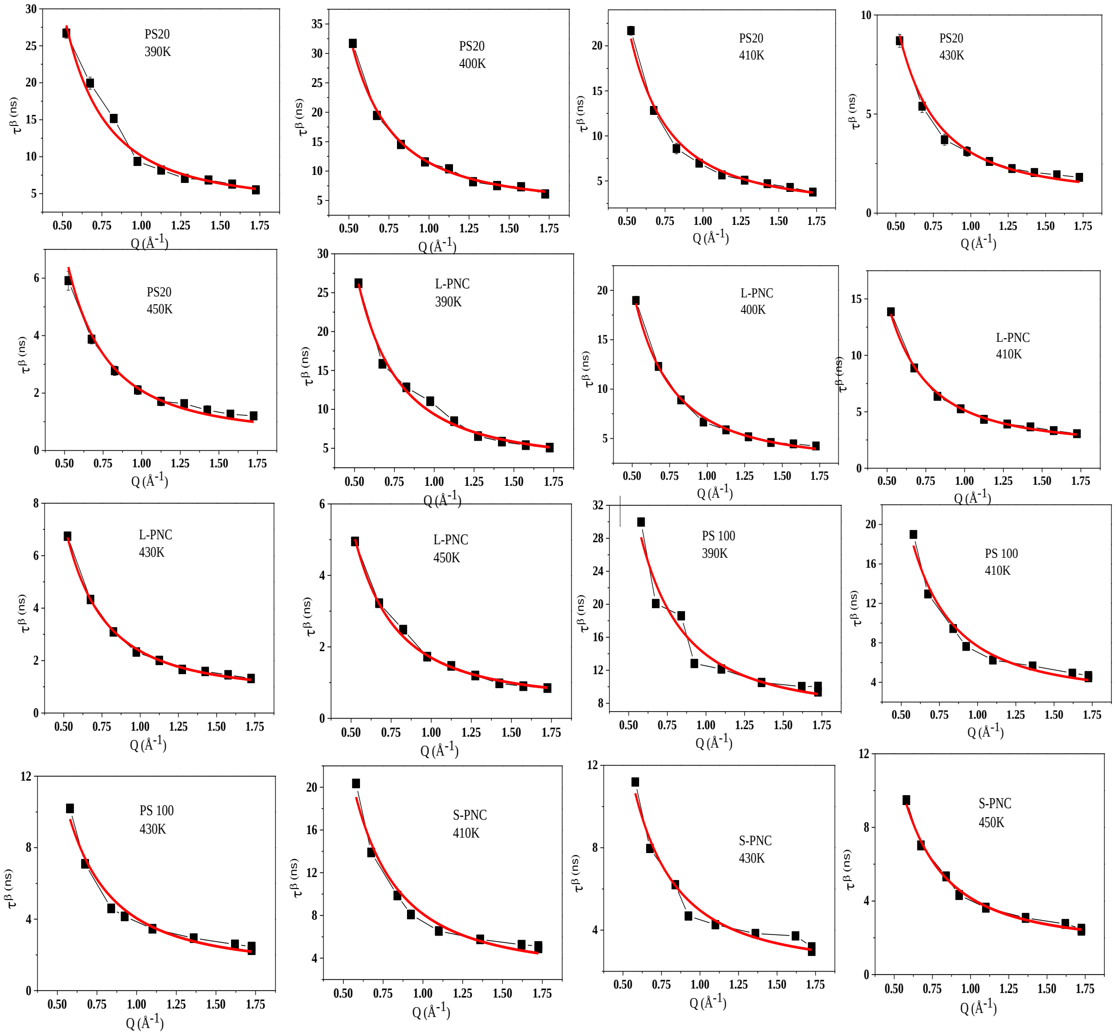

Fig. S8: $\tau^{\beta}_{\mathrm{kww}}$ vs Q with fits using jump-diffusion model (solid line) for all samples at all temperatures as specified in the legends.

Non-Gaussian Parameter from Anomalous Jump diffusion model

The amplitude $A(Q,t)$ extracted by modeling $I(Q.t)$ is shown in Fig. S9 (a-b) and (d-e). The solid red lines indicate the fits using Debye-Waller factor-like expression $A(Q,t) \approx \exp - [\frac{<u2>Q^2}{3}]$. The extracted mean squared displacement $< u^2 >$ for all the samples is shown in Fig. S9 (c) and (f). The $< u^2 >$ for L-PNC is more than PS20. Whereas, $< u^2 >$ for S-PNC is less than PS100.

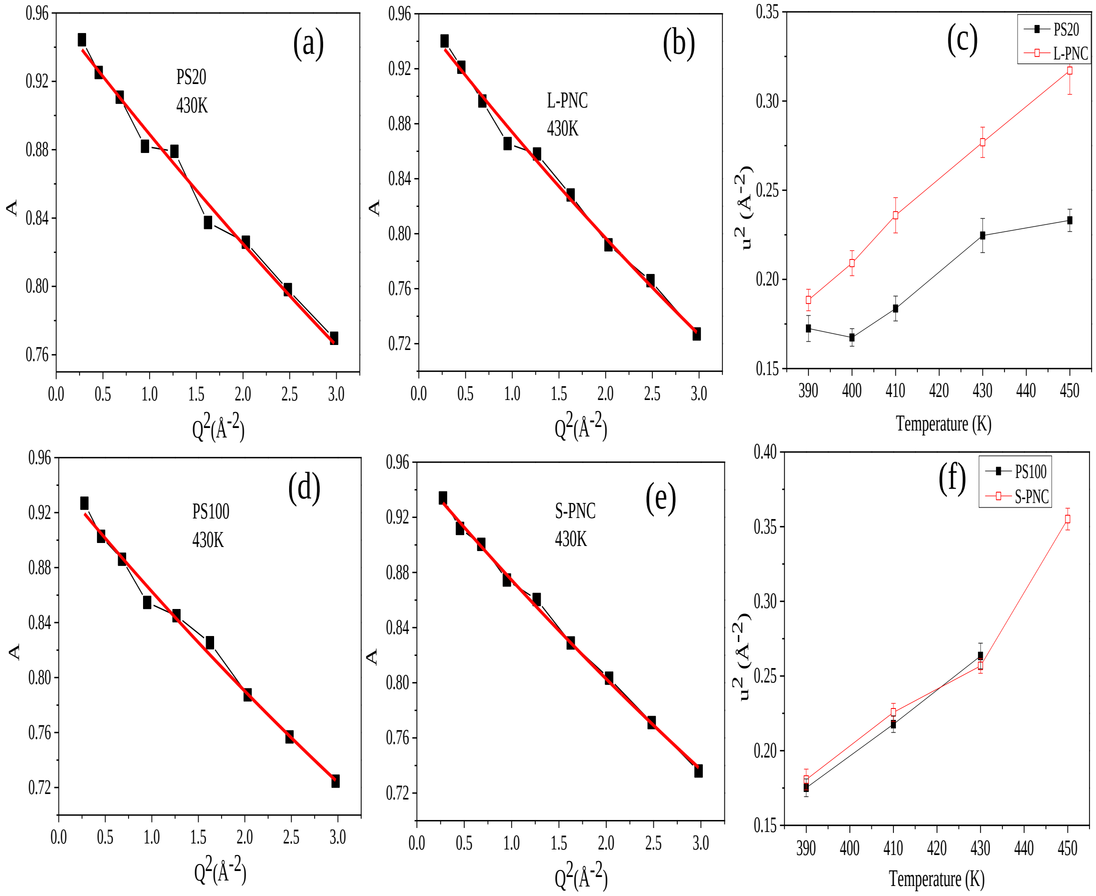

Fig. S9: $A(Q,t)$ vs Q fitted with Debye-Waller factor-like expression for a) PS20, b) L-PNC, d) PS100, and e) S-PNC at $T = 430$ K (The solid line represents the fits). The extracted mean square displacement $< u^2 >$ vs temperature for (c) high f and (f) low f samples with respective pristine polymers.

The dynamical heterogeneity (DH) is quantified by estimating the non-Gaussian parameter, α_2 using,[5]

$$\alpha_2(t) = \frac{72 l_0^4 (\frac{t}{\tau_0})^\beta}{[2u^2 + 6l_0^2((\frac{t}{\tau_0})^\beta)]^2}, \tag{1}$$

where l_0 and τ_0 are taken from the jump-diffusion model and the mean squared displacement $< u^2 >$ is extracted from the model fits of amplitude $A(Q,t)$ (Fig. S9). The α_2 for all samples at different temperatures are shown in Fig. S10. The non-Gaussian parameter is reduced with temperature indicating a reduction in DH with an increase in temperature.

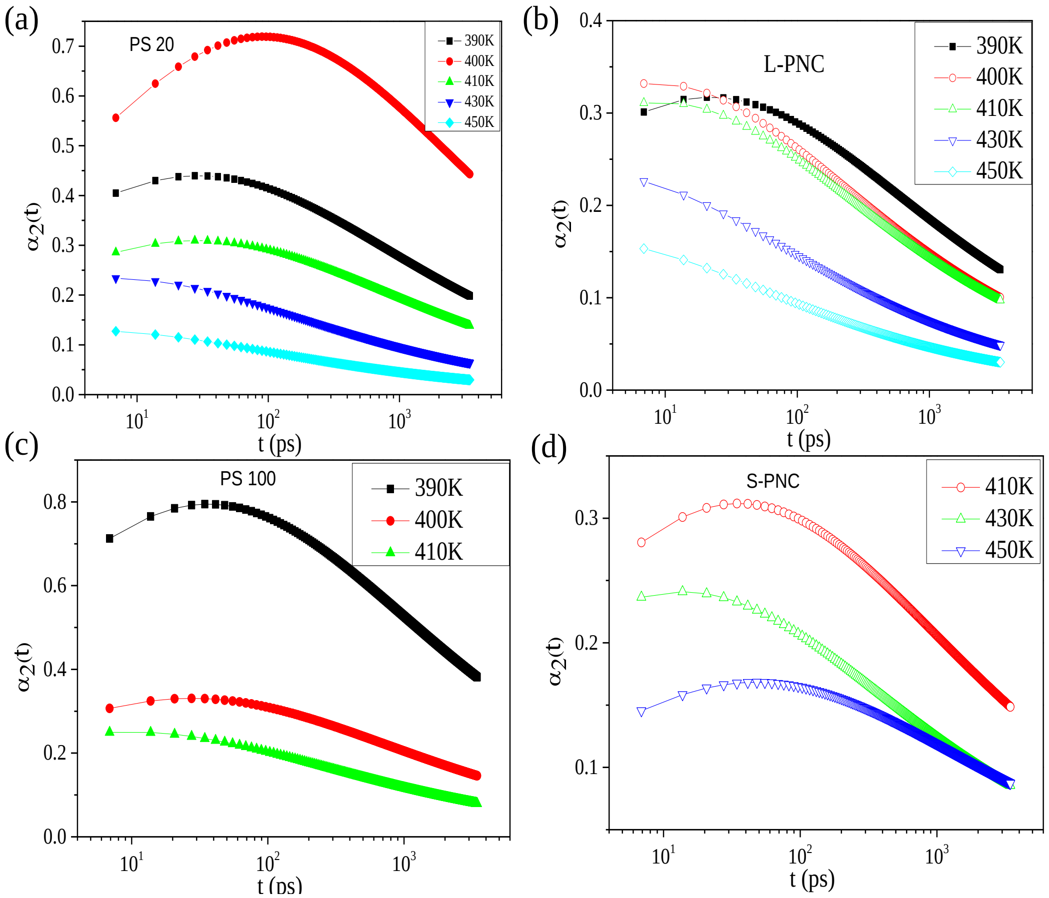

Fig. S10: The non-Gaussian parameter, α_2 for various temperature for a) PS20, b) L-PNC, c) PS100, and (d) S-PNC.

References

(1) Swain, A.; Begam, N.; Chandran, S.; Bobji, M.; Basu, J. K. Engineering interfacial entropic effects to generate giant viscosity changes in nanoparticle embedded polymer thin films. *Soft Matter* **2020**, *16*, 4065–4073.

(2) Das, N.; Begam, N.; Ibrahim, M.; Chandran, S.; Padmanabhan, V.; Sprung, M.; Basu, J. K. Viscosity and fragility of confined polymer nanocomposites: a tale of two interfaces. *Nanoscale* **2019**, *11*, 8546–8553.

(3) Gundlach, N.; Hentschke, R. Modelling filler dispersion in elastomers: relating filler

morphology to interface free energies via SAXS and TEM simulation studies. *Polymers* **2018**, *10*, 446.

(4) Arnold, O.; Bilheux, J.-C.; Borreguero, J.; Buts, A.; Campbell, S. I.; Chapon, L.; Doucet, M.; Draper, N.; Leal, R. F.; Gigg, M., et al. Mantid—Data analysis and visualization package for neutron scattering and μ SR experiments. *Nuclear instruments and methods in physics research section a: accelerators, spectrometers, detectors and associated equipment* **2014**, *764*, 156–166.

(5) Arbe, A.; Colmenero, J.; Alvarez, F.; Monkenbusch, M.; Richter, D.; Farago, B.; Frick, B. Non-Gaussian nature of the α relaxation of glass-forming polyisoprene. *Physical review letters* **2002**, *89*, 245701.

(6) Arbe, A.; Colmenero, J.; Alvarez, F.; Monkenbusch, M.; Richter, D.; Farago, B.; Frick, B. Experimental evidence by neutron scattering of a crossover from Gaussian to non-Gaussian behavior in the α relaxation of polyisoprene. *Physical Review E* **2003**, *67*, 051802.